IAC-11.B2.2.8

SPACE COMMUNICATIONS PROTOCOLS FOR FUTURE OPTICAL SATELLITE-DOWNLINKS

Dirk Giggenbach
German Aerospace Center, Germany, dirk.giggenbach@dlr.de

Florian Moll, Christian Fuchs, Tomaso de Cola, and Ramon Mata-Calvo
German Aerospace Center, Germany
florian.moll@dlr.de, christian.fuchs@dlr.de, tomaso.decola@dlr.de, ramon.matacalvo@dlr.de

As telemetry downlink data rates from EO-satellites increase and available radio frequency transmission spectrum narrows, optical data downlinks based on directed modulated laser sources become a beneficial alternative. While solving the bottleneck of data rate by providing licensing-free transmission at up to multi-Gigabit per second data rates, the required onboard terminal hardware is at the same time small and uses low transmit power. However, the transmission channel is very different to RF downlinks as new atmospheric effects have to be regarded, mainly cloud blockage, increased attenuation at low elevations, and index of refraction turbulence. To enable also with optical downlinks the level of global cooperation prevailing in RF downlink operations, it is necessary to elaborate and standardize optimized optical transmission formats. We present here the characteristics of optical LEO downlinks and the requirements they impose on the transmission data formats and protocols. We consider how existing RF satellite transmission-securing formats can be adopted and extended to enable reliable and efficient optical downlinks.

I. INTRODUCTION

Direct optical satellite downlinks for earth observation telemetry data have been tested with experimental and prototype systems [1,2]. This technology has the potential of boosting downlink throughput by several orders of magnitude compared to current RF-links by increasing the data rate of the downlink signal to multi-Gigabit/s. At the same time, power consumption, mass and volume of the optical transmit terminal on board the satellite can be dimensioned very beneficially. This is done by making use of the asymmetric link scenario, where a larger ground receive telescope of the optical ground station (OGS) can make up a large fraction of the link budget, allowing small and lightweight transmit telescopes on the satellite side. The potential performance of such systems has been presented in [6].

Optical satellite-ground links (OSGL) is a high-directivity point-to-point link technology and bears characteristics which are completely different from those known from the RF channel:

- Atmospheric attenuation of laser signals increases at low elevations, causing a high overall link dynamic of mean received power.
- Link-blockage by clouds has to be regarded:
  - long-term (complete blockage of an Optical Ground Station by cloud cover during an over-flight)
  - short-term (transitional blocking by small clouds during one downlink).
- Scintillation of Rx-power: in contrast to RF-links, optical downlinks feature very small scale amplitude scintillation patterns (cm to dm size) caused by atmospheric index-of-refraction turbulence (IRT). This leads to fast fades and surges (in milliseconds-range) of the received optical power of typical up to +/-6dB in the downlink and more in the uplink.
- With the extremely narrow optical beam, residual pointing errors from the space terminal can cause an additional source of fading.
- Depending on the modulation format and the applied receiver technology, further impacts onto the signal stability due to IRT have to be regarded. However, by limiting our treatment here to simple direct detection systems with multi-mode receivers, only Rx-power scintillation as already mentioned must be considered in terms of IRT effects.

As a typical behaviour of Rx-power in an optical LEO downlink, Fig 1 shows KIODO-2006 (KIrari Optical Downlink to Oberpfaffenhofen) trial #4 which took place between JAXA's *Kirari* satellite and OGS-OP at Oberpfaffenhofen near Munich on June 15th 2006 starting at 23:51 UTC. Tx-power from Kirari was kept constant during the downlink, the increase of Rx-power between 2.5° and 24° was thus purely due to the reduction of free space loss and atmospheric attenuation with increasing satellite elevation. Above 24° a cloud hindered the further increase of Rx-power. The six short breaks visible in the mean Rx-power were due to a deterministic behaviour of the satellite terminal's

pointing mechanism. Note that the received power was unusually high for a LEO downlink as the Tx-terminal onboard Kirari was designed for inter-satellite links and thus had an even more narrow divergence than it would be the case in future OSGLs. An overview of all 5 successful KIODO2006-downlinks can be found in [1]. The lower graph in Fig 1 shows the scintillation of Rx-power caused by the IRT. This scintillation-behaviour can vary strongly due to varying meteorological conditions during the downlink.

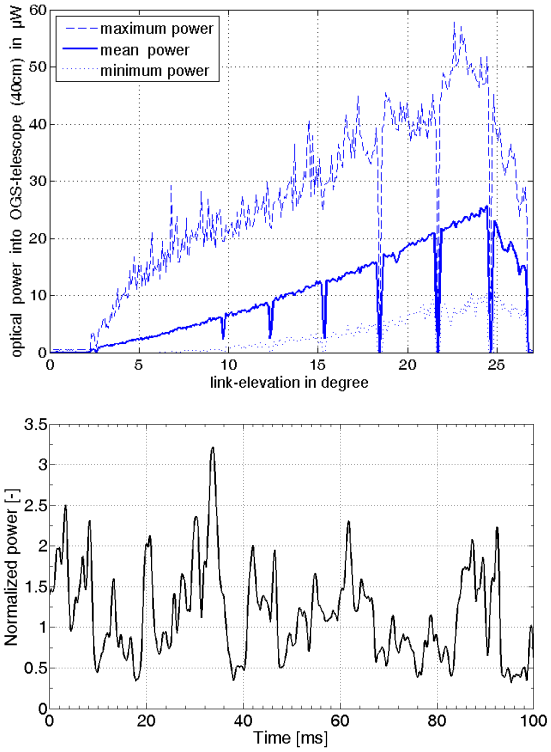

Fig 1: Typical received optical power at OGS measured during one of the first experimental optical LEO downlinks. OGS aperture diameter was 40cm, Tx-wavelength 847nm, Tx-power from sat-terminal was 100mW. Upper plot: typical received power over elevation (min., mean, and max. of each second). Lower plot: 100ms of typical short term Rx-power scintillations at 10° elevation due to index-of-refraction turbulence (normalized to mean value of one).

Further to be taken into account is the availability of a return channel: As in optical downlink systems typically the ground station illuminates the satellite terminal with a laser beacon to enable precise pointing, this beacon can also be modulated and used as an ARQ return channel. Such a bidirectional link – also if highly asymmetric in data rate – enables very efficient and reliable data transfer also in lossy channels.

Based on in-situ measurements of several optical LEO downlink trials and by applying channel models, requirements are defined for the adaptation of existing and the implementation of new transmission formats and protocols. Regarding the modulation-format, we focus on Intensity-Modulation / Direct-Detection as a robust and cost-effective format especially for LEO-downlinks.

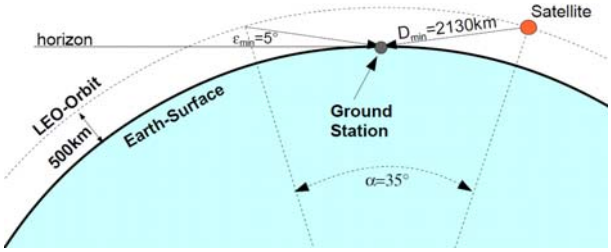

Fig 2: Reference LEO downlink geometry: 500km altitude near-polar circular orbit.

For the further investigations in this section we define a typical reference scenario for optical LEO-downlinks (Fig 2). As a reference satellite orbit we use here the typical EO-LEO in circular near-polar orbit (96° inclination) at 500km altitude, Tx-wavelength is 1550nm. Example ground stations are at Svalbard, OGS-OP at Oberpfaffenhofen near Munich, and Singapore as an OGS near the equator.

The satellite mean visibility (V_{sat}) over elevation angle for the three OGS are shown in Fig 3. Obviously, low elevations (below 20°) make up the major part of contact time.

OGS	**Svalbard**	**Munich**	**Singapore**
Latitude	78.2167°	48.0821°	1.33°
Longitude	15.3833°	11.2755°	103.83°
Total V_{sat} (0°-0° / 5°-5°)	11.35% / 7.99%	3.92% / 2.43%	2.30% / 1.45%
V_{sat} per day (0°-0° / 5°-5°)	163.4 / 115.1min	56.4 / 35.0min	33.1 / 20.9min
V_{sat} per contact (0°-0° / 5°-5°)	10.4 / 7.3min.	9.1 / 7.3min.	9.0 / 7.2min

Table 1: Reference ground stations for the following visibility and throughput considerations. Visibility is purely geometrical (elevation angle >0° and >5° respectively), not regarding link blockages by clouds.

The ordinate in Fig 3 represents the probability that the elevation is below a certain value. The values are normalized to the ground station Svalbard, which has the highest geometrical contact time due to its geographical location. During roughly 50% of time, the contact to the satellite remains below 10° elevation, for all three OGSs.

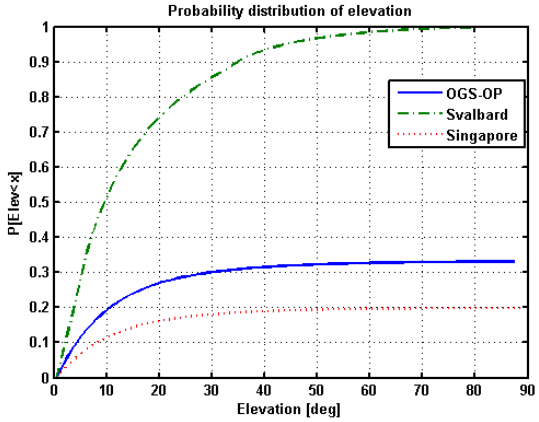

Fig 3: Probability-distribution-function of pure geometrical visibility for the reference LEO orbit, for three ground stations (Svalbard, OGSOP, and Singapore). Y-axis represents the visibility percentage respect to Svalbard.

We can deduce a relative datarate versus elevation, as shown in Fig 4, when taking into account the following assumptions:

- received power is linear to (1/range^2), with the range being a function of elevation only (circular orbit)
- transmittable data rate is linear to received power
- clear-sky atmospheric signal attenuation a_{atmos} in dB down to an OGS situated 100m above sea level can be modelled according to formula (1), which we use here for λ=1550nm.

In the left axis of the Fig 4, the bit rate is normalized to the zenith. It represents the reduction of the bit rate when decreasing the elevation. If we assume a maximum bit rate of 10Gbit/s at zenith, the right axis shows the bit rate change with the elevation.

Finally this relation allows us to plot a distribution function of the relative throughput versus minimum systematic link elevation angle, for our three OGS-locations, as depicted in Fig 5.

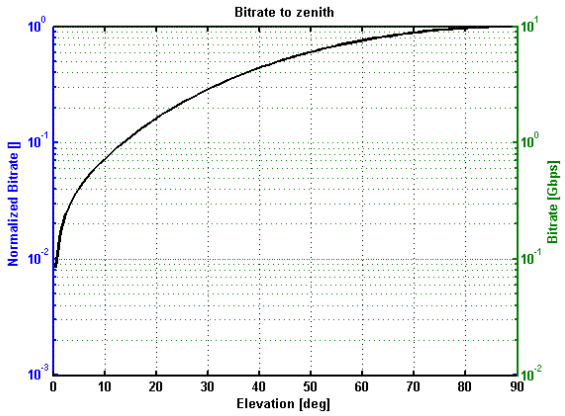

Fig 4: Transmittable data-rate based on mean received power (scintillations not taken into account here) as a function of elevation for our reference scenario.

Again the values take Svalbard as reference with the ordinate normalized to one at zenith.

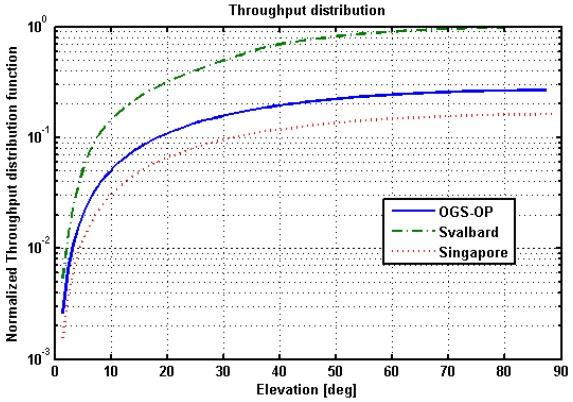

Fig 5: Distribution function of throughput for the three OGS locations, considering the orbit from fig 2, the attenuation over elevation (at 1550nm signal wavelength) according to (1) and a perfectly variable data rate that is linear to received power. Throughput is normalized to Svalbard, the ordinate represents the percentage of throughput with respect to this OGS.

Fig 5 illustrates that - although the data rate is much lower at low elevations due to the increased free-space loss and atmospheric attenuation - low elevations provide a significant fraction of the total downlink capacity. A technical necessary minimum elevation of 5° only causes negligible throughput loss compared to 0° minimum elevation as noted in table 2.

OGS	Svalbard	Munich	Singapore
Throughput- fraction below 5°	5.2%	7.4%	7.4%
Minimum elev. for 50% throughput	30.25°	24.8°	24.8°
Total mean daily throughput above 0°	13.1Tbit	3.5Tbit	2.1Tbit
Total mean daily throughput above 30°	6.6Tbit	1.4Tbit	0.9Tbit
Total mean daily throughput above 5°	12.4Tbit	3.2Tbit	1.9Tbit

Table 2: Upper row shows the fraction of data throughput lost by the systematic minimum elevation of 5°, second row gives the minimum elevation for a throughput loss of 50°, further rows give the average daily throughput for different minimum elevations. The system has perfect data-rate adaptation to Rx-power over elevation. *All values not regarding the effect of cloud blockage.*

Besides increased throughput, low elevations enable a less fragmented data flow (more downlinks, longer downlinks).

Therefore transmission systems for optical LEO downlinks must be able to work under low elevations and must be able to adapt their effective data rate accordingly (by varying channel data rate, modulation format, and FEC-overhead).

II. THE ATMOSPHERIC OPTICAL SATELLITE-GROUND COMMUNICATIONS CHANNEL

For estimation of channel behaviour, models and measurements of path attenuation and influence of optical turbulence can be used. In this section, total path attenuation is modelled by the approximation (1) [3] and turbulent behaviour can be estimated with example measurements. These were undertaken during the measurement campaign KIODO (KIrari Optical Downlink to Oberpfaffenhofen) in 2006 [1] and 2009 [4].

The total path attenuation is a fairly controllable issue, whereas the turbulent behaviour is a big challenge. The later one together with the possibility of clouds blocking the link are basically the two major impairments to overcome when dealing with optical satellite downlinks. Many studies with cloud occurrence statistics have been published to estimate the availability of a satellite-ground optical communication system, like [5,6,7]. For a single station in southern Europe, especially the Mediterranean region, availabilities between 66% and 84% annual average for a single station are realistic. To boost this value towards 100%, the cloud blockage effect can be mitigated by applying multiple ground stations in meteorologically uncorrelated locations. Thus, availabilities approaching 99% over the year are possible, for instance by using four stations [5,8]. When a ground station network is applied, data is sent to Earth via that OGS which is obscuration free. Since the satellite will not see all station at once, it is necessary to have a certain storage capacity on board to buffer data and resend it when overflying an unobscured ground station.

II.I Total downlink path attenuation as a function of elevation and wavelength

Clear-sky (i.e. no clouds) atmospheric signal attenuation down to an OGS roughly depends on elevation ε (in degree) and signal wavelength λ. In [3] a simple model for OGSs situated 100m above sea level is given for λ=[850nm/1064nm/1550nm] (outside of atmospheric molecular absorption bands), which here is represented as approximation (1).

$$a_{atmos}(\varepsilon) = \frac{10}{\left(\frac{\lambda}{1550nm}\right)^{2} \cdot (\varepsilon + 1)} dB \qquad (1)$$

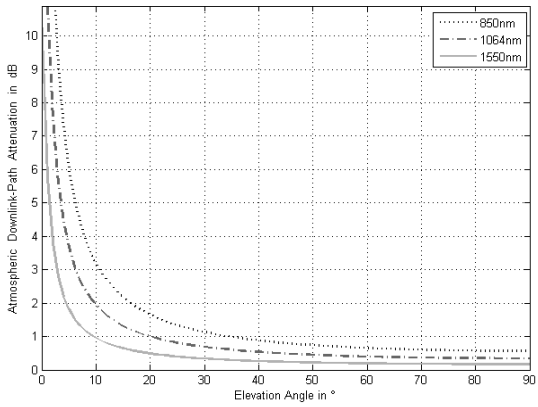

Fig 6: Atmospheric attenuation in space downlinks for three typical data-com laser wavelengths, as a function of path elevation. Below 20° elevation, the atmospheric attenuation becomes a major loss factor. Taken from [3].

Below, Fig 7 shows an estimate of the global cloud condition. The statistics are based on data from the International Satellite Cloud Climatology Project (ISCCP). It depicts the total cloud amount averaged over the year. Regions with low values are preferable. However, issues like local turbulence strength and infrastructure are also important for OGS site selection.

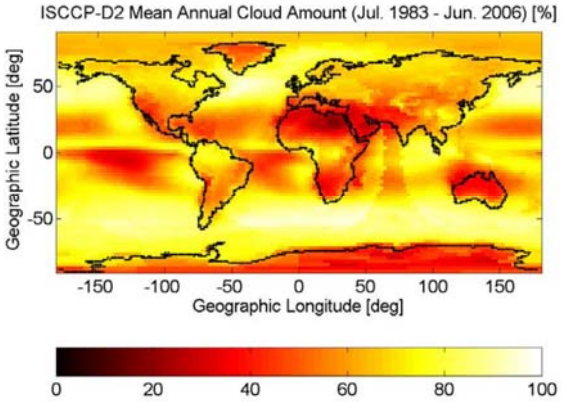

Fig 7: Mean annual cloud coverage for the time from July 1983 to June 2006 based on data from the International Satellite Cloud Climatology Project (ISCCP). The colour indicates the amount of mean cloud coverage from black = 0% over red, orange and yellow to white = 100%. Taken from [9].

II.II Power Scintillation Index

Atmospheric turbulence has a strong impact on link performance. The index of refraction turbulence (IRT) along the link path causes the beam to interfere constructively and destructively. Therefore, a speckle pattern in the beam cross section, which changes in space and time, evolves. This pattern, when received with a finite aperture, causes the received signal to fluctuate around a certain mean value.

A common way to describe the signal fluctuations in free-space optical communication systems is the Power Scintillation Index (PSI). An in-depth explanation can be found in various publications, e.g. [10]. The PSI is calculated with

$$\sigma_p^2 = \frac{\langle P^2 \rangle - \langle P \rangle^2}{\langle P \rangle^2} \qquad (2)$$

Different to the intensity scintillation index, it takes into account the averaging effect of the receiving telescope aperture. Increasing aperture diameters cause lower power fluctuations and thus, less fading. In Fig 8, the PSI for the LEO downlinks of the KIODO trials is depicted. With higher elevation angles, the fluctuation is reduced significantly. The records of all seven measurements show similar runs. However, certain variability persists due to different atmospheric conditions.

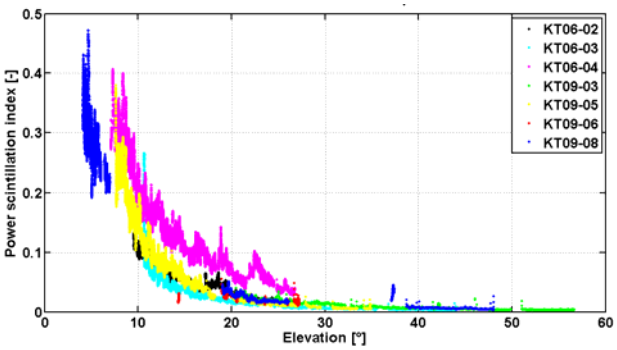

Fig 8: Plot of power scintillation index as recorded for different downlinks of the KIODO-experiments.

An interesting effect is the saturation of scintillation for very low elevations. Although the optical path length through the atmosphere gets longer at these elevation angles, the PSI and thus the signal fluctuations observed at the receiver become smaller. This effect is especially visible in two measurements in the uplink channel shown in Fig 9. Furthermore, PSI is somewhat higher than in the downlink due to nonexistence of aperture-averaging. Reason is that the satellite terminal's telescope is smaller than intensity speckles in the uplink. This observation illustrates also the asymmetry of the satellite-ground channel.

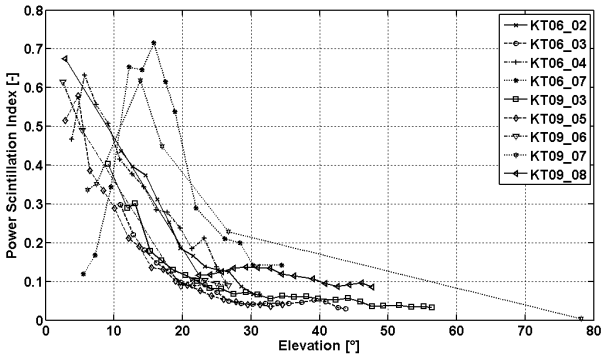

Fig 9: Plot of PSI as observed for the Uplink of all KIODO Experiments. Two parallel beacon lasers were used during all experiments (→ see *Tx-diversity*, below).

II.III Signal fading in downlink

In this section, the problems arising from strong downlink power fluctuations are discussed. Fig 10 illustrates the instantaneous high dynamics which may be as large as 20dB for low elevation angles. The dashed line marks a 3dB-threshold from elevation-normalized mean which defines a fade. This 3dB-threshold is also used in the forthcoming analysis. As one might expect, fades vanish with growing elevation.

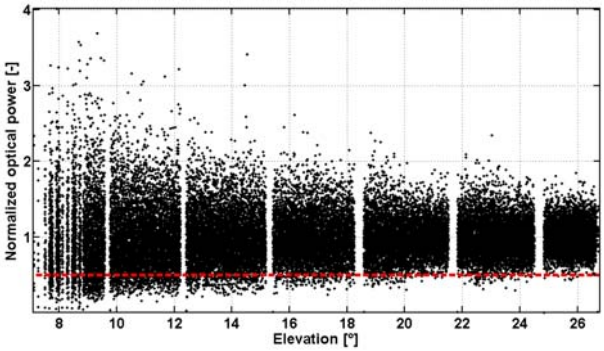

Fig 10: Normalized power for an example downlink. A fade is assumed if power drops below 3dB of the mean (marked by dotted line).

With receiver aperture sizes bigger than the 40cm used in this measurement, these fluctuations can be further reduced (aperture averaging). However, since ground stations are likely to have aperture sizes within this range, the communication system has to cope with these strong fluctuations.

In Fig 11-13, fading behaviour and channel characteristics are depicted over link elevation. Because with rising elevation the link path through the atmosphere becomes shorter, the influence of atmospheric turbulence weakens and therefore, fading becomes weaker. Here, fading is defined to occur, if power drops 3dB below the instantaneous mean power. The fade number per second is shown in Fig 11. Fades may occur quite often within low elevations, i.e. more than 100 times per second and become quite seldom for high elevations.

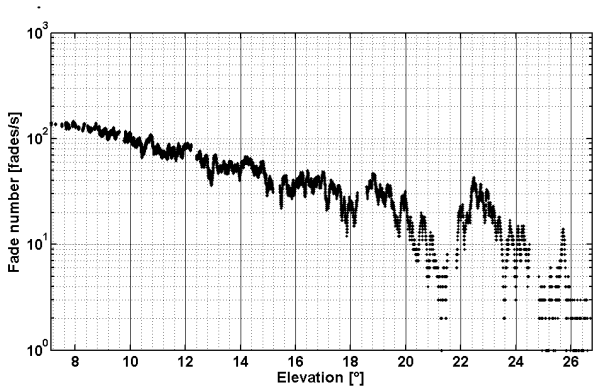

Fig 11: Fade frequency for an example downlink. A fade is assumed if power drops below 3dB of the mean.

The fractional fade time in Fig 12 defines the percentage of time the received power is below the threshold. At lower elevation, this can reach over 20% of time, decreasing to below 1% for higher elevations.

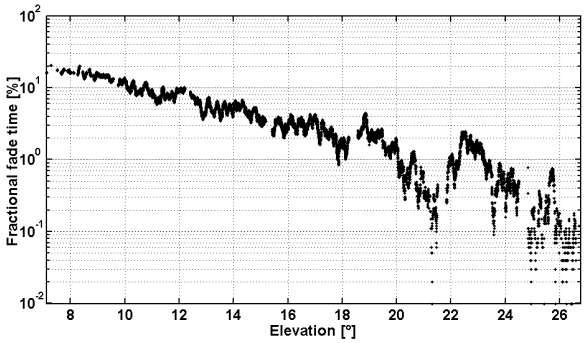

Fig 12: Fractional fade time over elevation for an example downlink. A fade is assumed if power drops below 3dB of the mean.

The mean fade duration is important to estimate number of data packets within a fade and is depicted in Fig 13. Depending on link elevation the mean fade time lies between 0.2ms and 1.6ms.

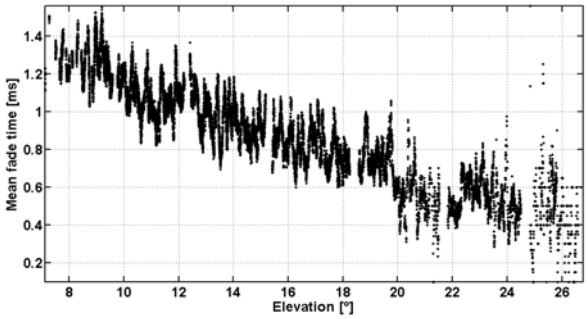

Fig 13: Mean fade time over elevation for an example downlink. A fade is assumed if power drops below 3dB of the mean.

The mean fade time has the same order of magnitude like the received power auto-correlation time (ACT) as illustrated in Fig 14. Here, this correlation time is defined as the 3dB roll-off point in the concerned normalized auto-covariance function. Therefore, it is the functions half width at half maximum. However, the qualitative behaviour of the ACT is different to those of the mean fade time. Whereas the later decreases monotonically, the ACT first increases up to a certain maximum and then decreases. The explanation is the counteracting of two different phenomena. The first is the fact that with longer link paths, turbulence is stronger and thus correlation time shorter. The second is the slew rate of the satellite, which is quite slow at small elevation angles and relatively fast at high elevations. These two effects work against each other whereas during link time, the first dominates at low elevations and the second at higher.

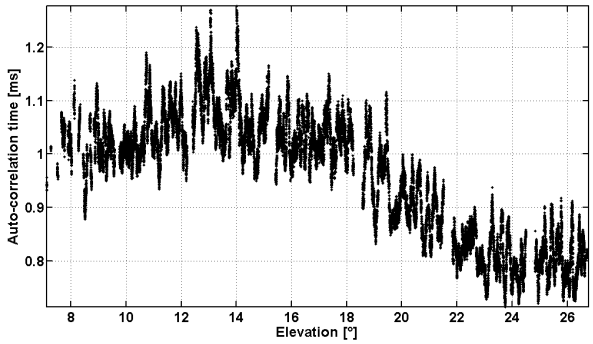

Fig 14: 50% atmospheric correlation time over elevation for an example downlink.

For the actual measurements are undertaken with a wavelength of 847nm, they have to be translated to other wavelengths if necessary by the use of appropriate models. In [11], the intensity correlation width is found to behave approximately proportional to wavelength in the case of weak turbulence, i.e. link elevations over 10°. Furthermore, Taylors frozen turbulence theory can be applied, which gives the possibility to relate spatial to temporal statistics [10]. Now, assuming those models to be valid, the correlation time is found to scale linearly with wavelength. Thus, the time dimensions in Fig 14 can be converted to other wavelengths. For instance, the correlation time being between 0.65ms and 1.4ms for 847nm in Fig 14 could lie in the range 1.2-2.6ms for 1550nm.

II.IV Signal fading in uplink

As far as the downlink is concerned, fading effects can be mitigated by using a larger telescope and thus exploiting the aperture averaging effect [12]. As the size for an optical terminal onboard a satellite and thus the aperture size are limited, this effect is not applicable in the same manner for a satellite uplink. The solution is to use several beacon lasers (Tx-diversity), separated by a larger distance than the atmospheric coherence length r_0 at the corresponding ground station site. During all KIODO Trials, two beacon lasers were used.

Fig 15 shows the normalized power obtained during the experiment. Due to the lower sampling rate onboard the satellite the data point density is lower as for the previous plots of the downlink. Also in the uplink it is visible that the fading gets lower as the elevation angle is increasing during a satellite-pass. The dynamic range of the uplink-signal is, although in the same order of magnitude, larger as for the downlink.

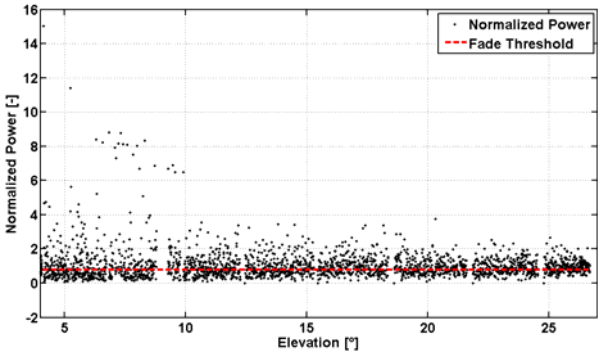

Fig 15: Normalized power over elevation for an example uplink. A fade is assumed if Rx-power at satellite drops below 3dB of the mean.

Fig 16 shows the fade frequency, i.e. the number of fades observed in one second. At low elevation angles, fades may occur as often as 180 times per seconds, reducing to some ten fades per second at higher elevation angles.

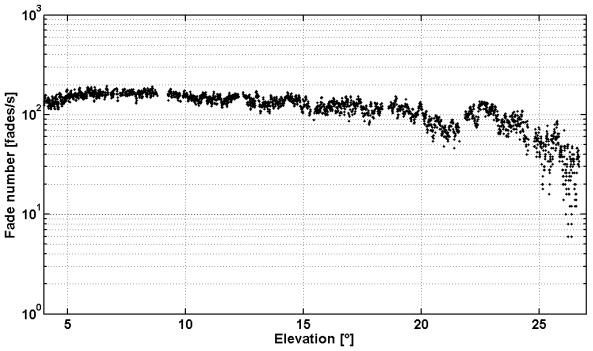

Fig 16: Fade frequency over elevation, uplink.

Fig 17 shows the fractional fade time measured in the uplink. For low elevations, it peaks at a value as high as 35%, meaning that fades are observed 35% of the time. This indicates that strong FEC coding, capable of recovering packet-loss in the order of 35…40%, needs to be applied to enable a reliable uplink.

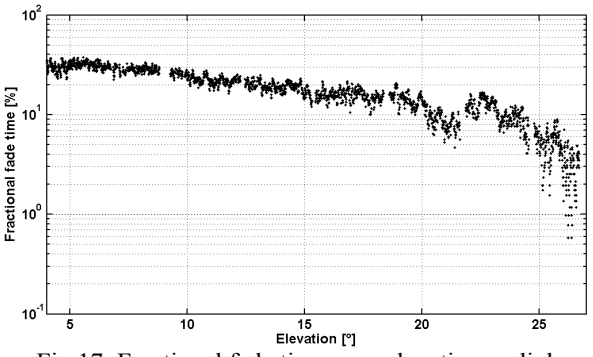

Fig 17: Fractional fade time over elevation, uplink.

Fig 18 shows the mean duration of the observed fades. Fades may have a length of around 2.5 ms at low elevation angles. This duration drops to a value of 1 ms at higher elevations in this measurement.

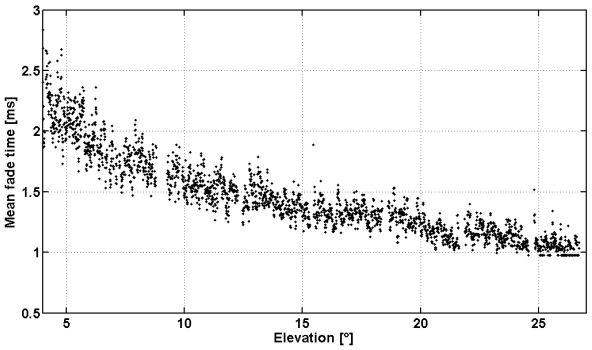

Fig 18: Mean fade time over elevation for an example uplink.

Fig 19 finally shows the atmospheric correlation time in the uplink. It peaks at values around 2 ms at low elevation angles and gets down to between 1.5 and 1.0 ms at higher link elevations.

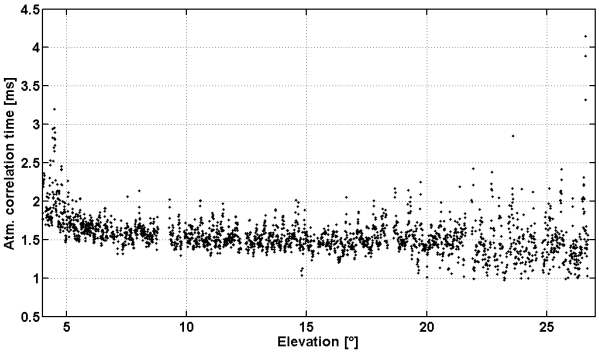

Fig 19: 50% atmospheric correlation time over elevation for an example uplink.

From the previous plots it is visible that the fading behaviour in the uplink seems slightly worse compared to the behaviour in downlink direction, although all parameters remain in the same order of magnitude. It has to be regarded that Tx-diversity (2 beacon lasers from OGS) was used, which reduces fading and thus lead to a comparable behaviour in the uplink, although no aperture averaging like in the downlink takes place in the uplink. Additional exploitation of Tx-diversity (e.g. 4 instead of 2 beacon lasers) might be a way to further improve the statistical behaviour in uplink direction.

Another valuable consideration is to use an uplink with only a low data-rate (in the order of Mbit/s). This is sufficient for e.g. the transmission of repeat requests and the exchange of other telemetry like channel status information. Due to the lower bit rate, the quantity of lost bits during one fade is remarkably lower and thus other criteria are relevant for the code design in the uplink. As en example, the mean fade time as visible in Fig 18 indicates fade lengths of around 2.5 ms at low elevation angles. Taking into account a bit rate of 1 Mbit/s, a quantity of 2500 bits is lost in one fade, which can be recovered by standard interleaved FEC. In contrast to this, the quantity of lost bits is much higher in downlink direction: With the mean fade time of around 1 ms in Fig 13 and a bit rate of 10 Gbit/s, 10 million bits are lost during one fade. This indicates that only FEC schemes with very long influence lengths are appropriate for the coding in downlink direction.

III. SUMMARY OF THE BOUNDARY CONDITIONS IN OSGL AND REQUIREMENTS FOR THE DATA-SECURING MECHANISMS

As shown in the previous sections, an optical downlink system must be able to cope with a variety of channel characteristics that are very different to those known from RF downlinks. In summary these are:

- Increased elevation-dependent mean Rx-power dynamic due to range-loss plus atmospheric attenuation loss. As low elevations are crucial to achieve a high overall throughput, means to cope with this dynamic are required. These means will be mainly *adaptive data rate and adaptive AWGN-FEC-overhead*, both changing with elevation.
- Received power scintillation strength caused by IRT depends on a set of geometrical and meteorological constraints as there are:
  - meteorological conditions at OGS-site
  - Rx-aperture diameter
  - wavelength
  - receiver technology
- The received power fading caused by IRT depends also on elevation and thus requires again *dynamic FEC overhead for fading mitigation* (which generally will rely on different mechanisms than the AWGN-FEC).
- Also the duration of fades depends on elevation and the other parameters already mentioned above. Together with the high channel data rate this will heavily influence the dimensioning of interleavers, which need to be able to cope with gigabits of memory.
- Short-term link blockages by transient link loss and single clouds require a suitable ARQ protocol.
- Long-term cloud blockages that completely hinder single downlinks again require delay tolerant networking technologies.
- Another source of fading could be the tracking- and pointing-quality of the space- and ground-

terminals. However, this should be a solvable problem as other opto-mechanical systems in space have proven that the impact of tracking errors can be reduced to negligible values.

- An optical *uplink*-beacon will be available in most cases, which can be used…
  - for channel sounding, allowing identification of link-loss or mean power reduction due to e.g. thin clouds. This information can be used to steer retransmission, data rate, or FEC-overhead
  - as a low-rate return channel for ARQ-protocols. However as this uplink will be susceptible to the same or even stronger scintillations as the downlink, according correction measures (FEC) need to be undertaken.

Approximate typical values for the channel parameters in future optical LEO downlink system are given in table 3.

Parameter	Minimum	Typical	Maximum
typical data rates	100Mbps	1Gbps	10Gbps
dynamic of mean Rx-power from 5° elevation to zenith (no clouds)	17dB	20dB	23dB
Rx-power in zenith (at maximum), dl	3µW	10µW	30µW
power scintillation index, dl / ul (with Tx-diversity)	0.05 / 0.05	-	0.5 / 0.8
short-term dynamic of Rx-power, dl / ul, in dB	±2 / ±4	-	±6 / ±10
fract. fade time (-3dB), dl / ul, in %	1 / 1	-	20 / 30
mean fade time, dl / ul, in ms	0.4 / 1	-	1.4 / 2.5
number of fades, dl / ul, per second	10 / 10	-	200 / 200
blockage probability of an OSGL by cloud cover (annual mean for any global OGS-site)	20%	50%	80%

Table 3: Rough order for parameters in OSGLs. Assuming transmission wavelengths in the NIR, 1W Tx-power, modulation format IM/DD, 100µrad beam divergence from satellite terminal (corresponds to ~15mm Tx-aperture diameter), OGS-aperture between 25cm and 60cm, OGS altitude between sea level and 2000m. All fade values for a -3dB fade threshold. (dl: downlink, ul: uplink)

The parameters from table 3 must be used to dimension the set of FEC-mechanisms shown in Fig 20 to secure the link at physical level.

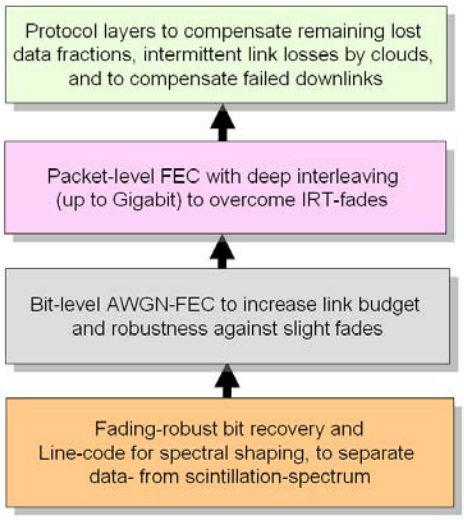

Fig 20: FEC mechanisms suitable for the fading optical satellite downlink channel.

IV. REVIEW OF SUITABLE EXISTING PROTOCOLS AND DATA FORMATS

The CCSDS (Consultative Committee for Space Data Systems) devised a dedicated protocol stack for space missions that can be considered as reference starting point also for supporting data communications in EO environments. CCSDS protocol stack actually defines all the protocol layers from the application down to the physical layer. In particular, some attention has to be dedicated here to the recovery options that are available in some protocol candidates.

According to recent standardisation activity being performed in the Delay Tolerant Networking (DTN) working group within CCSDS, space communications in next decade's space missions will implement a CCSDS/DTN protocol stack [13]. The Bundle Protocol (BP) and Licklider Transmission Protocol (LTP) [14, 15] are the core of the next-generation deep-space communication and for more general disrupted networking operations.

BP acts as overlay over the underlying protocol layers, thus allowing the implementation of dedicated protocols, depending on the characteristics of the applied environment. The philosophy of the BP is to de-compose the whole network in an internet of internets [16], through which data delivery is performed by

exploiting a store-carry-forward approach. BP implements a message-switching service: Application data units (ADUs) are encapsulated in the BP Data Units (BPDUs), commonly referred to as bundles. BP offers different encapsulation service towards the underlying layer, to ensure interoperability with different protocols, depending on the specific environment where the DTN architecture is applied. This is achieved by the so-called convergence layers, which allow BP to work over TCP [14], UDP, and LTP [17]. BP has the possibility to suspend and then resume a message delivery when a link is again available or when the quality is no longer degraded. To this end, dedicated mass memories have to be available in order to store all the incoming bundles during the message transfer interruption phase. A complimentary protection against bundle losses is the custodial transfer option, through which BP exploits the "mailman" principle. Nodes elected custodians (statically or through notifications) are responsible for forwarding bundles towards the next BP node. From a protocol implementation viewpoint, each custodian implements an ARQ mechanism to ensure that bundles are correctly routed to the next node.

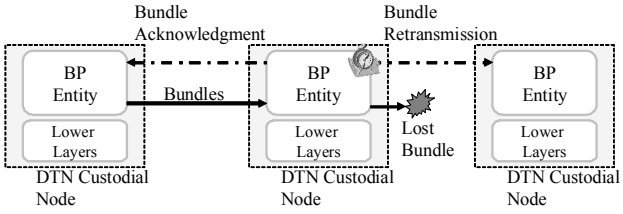

Fig 21: Custodial Transfer option and retransmission of a lost bundle upon bundle transmission timer expiration

As far as the Licklider Transmission Protocol (LTP) is concerned, it is implemented beneath the Bundle Protocol and is essentially a point-to-point protocol. LTP data units are usually referred to as segments and they handle data blocks forwarded by BP. Depending on the service requirements or the quality of service demanded by each block, LTP defines red and green parts for a given block. The former corresponds to parts which require to be delivered reliably, whereas the latter may require delivery immediacy. In order to properly handle these two types of profiles, LTP implements a NAK (Negative Acknowledgment)-based recovery scheme for red parts, whereas no protection mechanisms are enabled for the green. In particular, when LTP segments carry red parts, the retransmission of the missing parts is performed upon reception of a negative acknowledgment issued by the receiving LTP entity. The missed reception of a retransmitted segment is detected at the receiving side through NAK-timer expiration, triggering the issuance of a NAK to invoke a new retransmission loop.

Alternatively, it is also possible to consider other protocol solutions circulated in the literature and specifically designed for being operational in satellite scenarios. This is the case of the Saratoga [18] protocol, which is mostly a file transfer protocol developed to transfer image files from satellite to ground station in Earth Observation operations. It can be also used in conjunction with the Bundle Protocol. Its main value is actually to implement more efficient recovery mechanisms than TCP, although its applicability can be in fact limited to downlink transfers. Another possible candidate is the BuBa [19] protocol, whose design is however very close to that of LTP. Finally, attractive recovery functions are also offered by the NORM protocol [20], which implements NAK-based procedures to recover from information losses in multicast data transmissions.

Moving to the lower layers, different protocol solutions have been proposed by CCSDS in terms of datalink and coding and synchronisation sublayers. Particularly interesting is the CCSDS Proximity-1 protocol specification, which is shortly summarised in the following. The Proximity-1 protocol [21] is a 'Space Link Protocol' designed for the purpose of proximate communications among 'probes, landers, rovers, orbiting constellations, and orbiting relays'.

The Proximity-1 data services protocol provides two grades of service (Sequence Controlled and Expedited) [22] that determine how reliably Service Data Units (SDU) supplied by the sending user are delivered to the receiving user. The controlling procedure is called COP-P and consists of a Frame Operations Procedure for Proximity links (FOP-P), used on the sending side of the service, and a Frame Acceptance and Reporting Mechanism for Proximity links (FARM-P), used on the receiving side of the service. In few words, the Sequence Controlled service implement a go-back-n based ARQ strategy. As far as the coding specification is concerned, the (7,1/2) CCSDS convolutional code is employed, with a mandatory 32-bit CRC. Optionally, a concatenated (204,188) Reed-Solomon / (7,1/2) convolutional code is supported [23].

Finally, an interesting recovery option is represented by erasure coding, which is usually implemented as packet-level coding. Erasure codes can be actually implemented at any layer of the protocol stack. However, in virtue of the recovery mechanisms already available from the higher layers it is appropriate to think about erasure codes as a complimentary recovery means implemented right above the datalink layer. This way would allow the packet-level coding strategy to recover from packet erasures detected during short fading periods, whereas the ARQ schemes implemented at the

higher layer could be profitably used to retransmit the packets lost because of blockage or long fading events.

V. SUGGESTIONS FOR AN ADVANCED DATA FORMAT

The CCSDS protocol stack shortly illustrated in the previous section has been basically developed for space communications achieved with RF technology. As a consequence, its adoption for laser-optical based communication requires modifications and protocol re-configurations.

Particular attention has to be devoted to the transmission channel properties listed in Table 3. Physical characteristics play an important role mostly in the definition and specification of the datalink and physical layer, for what concerns the synchronisation and channel coding issues. Additionally, the frequency of fading events, their duration and the occurrence of signal blockage cases also influences the performance of upper layers, thereby requiring dedicated protocol tuning.

First, datalink and physical layer recommendations such as Proximity-1 are very much tailored to specific RF applications and therefore important modifications to the standard are required. These are particularly important for the frame length configuration and the design of the channel coding and synchronisation scheme. The latter is strictly connected to the level of robustness against link errors that has to be achieved in EO communications. Besides, the specific code design will definitely depend on the bit error patter and on the related stochastic characteristics. In turn, this choice also affects the length of the frame.

As to the upper layer protocol design, the required modifications are lighter as LTP and BP were designed to be technology independent and only their efficiency or behaviour can be differently influenced by the technologies being used. Conversely, the tuning of the protocol parameters and the overall protocol configuration plays here an important role. The erasure coding schemes have to be designed according to the average fading duration, the data rate and the on-board storage constraints. On the other hand, LTP could call for adequate tuning of the LTP segment transmission parameters and the related retransmission procedures. In particular, some attention should be devoted to the block aggregation performed before forming an LTP segment, which can differently condition the system performance. In fact, the appropriate choice of the LTP segment length according to the number of aggregated blocks is of fundamental importance to optimise the throughput and minimise the delay incurred in the data retransmission. Similar considerations also hold at the Bundle Protocol layer, for what concerns the bundle size and the overall management of the store/forward mechanism. In particular, much attention has to be also dedicated to the on-board memory actually used to store bundles when the link is not available (e.g., because of cloud coverage). In this light, fading durations in the order of few milliseconds (1-4 ms, according to Table 3) with frequency strictly depending on the data rate can be efficiently contrasted by the ARQ mechanism available within LTP or by the implementation of erasure codes. Actually, the case of 1 ms fading with data rate 100 Mbit/s gives rise to few packet losses (around 10, assuming a packet length of 1024 bytes), which can be easily and efficiently recovered by ARQ schemes. On the contrary, data rate 10 Gbit/s with fade duration 4 ms corresponds to thousands of lost packets (assuming again packet length 1024 bytes), for which the use of erasure codes could be more beneficial also in terms of required on-board storage and timely delivery of data to destination. On the other hand, blockage events which are inherently longer cannot be efficiently coped with by means of ARQ or erasure codes as their requirements cannot be easily accommodated (very large storage units). Under these circumstances, the use of store/forward capabilities as available from the Bundle Protocol is the most promising approach to not degrade the overall system performance and still offer a satisfactory degree of quality of service to the end-users.

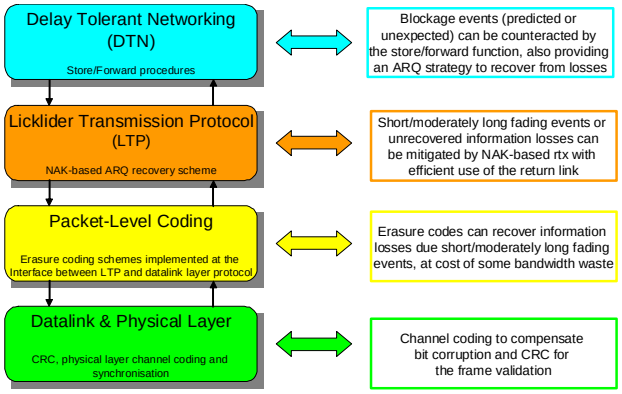

Fig 22: Protocol layer concept for the optical satellite downlink channel

VI. SUMMARY AND OUTLOOK

Measurements and models for the future optical LEO downlink technology indicate a high short-term dynamic due to index-of-refraction fading plus a high mean-power dynamic over elevation. While the short-term dynamic can be reduced somewhat by physical means like aperture averaging and Tx-diversity, receiver technologies must still be able to cope with a strong remaining dynamic to advantageously make use of the

channel capacity. Adaptive effective data rate over a 20dB Rx-power span is one requirement. This can be achieved either by directly varying data rate and thus bandwidth of the receiver and/or by adapting the FEC-overhead.

Channel sounding through the uplink beacon or even asymmetric two-way communications for ARQ-protocols will be other means for optimizing the link throughput and reliability.

Data-format like frame-length, synchronization, and inner and outer FEC encapsulation must be matched to the fading behaviour.

Protocol stack design should be essentially based on CCSDS standards, with the required configuration tuning to each protocol being involved. In particular, appropriate configuration of LTP segment size along with the bundle aggregation into bundles should be carefully taken into account with respect to duration of moderate fade events. Besides, the in-space storage requirements should be precisely figured out in order to trade-off the usual on-board storage constraints and the memory capacity required to perform retransmission procedures efficiently.

If dimensioned advantageously, direct optical satellite downlinks have the potential of revolutionizing EO-data-link technology, boosting the throughput even from small LEOs by orders of magnitude while reducing mass, size, and power constraints onboard the satellite.

We want to acknowledge the excellent cooperation with JAXA (Japan Aerospace Exploration Agency) and NICT (Japan National Institution of Information and Communication Technology) during the KIODO downlink campaigns in 2006 and 2009.

[1] T. Jono, Y. Takayama, N. Perlot, et al., "Report on DLR-JAXA Joint Experiment: The Kirari Optical Downlink to Oberpfaffenhofen (KIODO)", JAXA, ISSN 1349-1121, 2007

[2] B. Smutny, et al., "In-orbit verification of optical inter-satellite communication links based on homodyne BPSK", Proc. of SPIE 6877, 2008

[3] D. Giggenbach, "Mobile optical high-speed data links with small terminals", Proc. SPIE, Volume 7480, SPIE-Europe – Security and Defence, Berlin, Sept. 2009

[4] F. Moll, "KIODO 2009: Trials and analysis", in International Workshop on Ground-to-OICETS Laser Communications Experiments 2010: GOLCE 2010, 2010, pp. 161-171.

[5] F. Moll and M. Knapek, "Wavelength selection criteria and link availability due to cloud coverage statistics and attenuation affecting satellite, aerial, and downlink scenarios", in Proceedings of SPIE, vol. 6709, 2007

[6] D. Giggenbach, F. Moll, C. Fuchs, M. Brechtelsbauer, "Direct Optical High Speed Downlinks and Ground Station Networks for Small LEO Missions", in: Proceedings of the 16th Ka- and Broadband Communications Conference. 16th Ka- and Broadband Communications Conference, Milan 2010, 20.-22. Oct.

[7] F. Lacoste, A. Guerin, A. Laurens, G. Azema, C. Periard, and D. Grimal, "FSO ground network optimization and analysis considering the influence of clouds", in Proceedings of the 5th European Conference on Antennas and Propagation, 2011, pp. 2746 - 2750

[8] J. Horwath, N. Perlot; M. Knapek and F. Moll, "Experimental verification of optical backhaul links for high-altitude platform networks: Atmospheric turbulence and downlink availability", International Journal of Sat. Com.. and Networking, vol. 25, pp. 501-528, 2007

[9] D. Giggenbach, B. Epple, J. Horwath, and F. Moll, "Optical satellite downlinks to optical ground stations and high-altitude platforms", in Advances in mobile and wireless communications – views of the 16th IST mobile and wireless communications lecture notes in electrical engineering, vol. 16, 2008, pp. 331 - 349

[10] L. C. Andrews and R. L. Philips, "Laser beam propagation through random media", SPIE Press Bellingham, 2005.

[11] L. C. Andrews, R. L. Phillips, and C. Y. Hopen, "Scintillation model for a satellite communication link at large zenith angles", in SPIE Optical Engineering, Volume 39, pp. 3272 – 3280, 2000

[12] D. Giggenbach, H. Henniger, F. David, "Long-Term Near-Ground Optical Scintillation Measurements", in: Proceedings of the SPIE, Vol. 4976, LASE 2003, San Jose, USA

[13] "Rationale, Scenarios, and Requirements for DTN in Space. Rationale, Scenarios, and Requirements for DTN in Space", CCSDS 734.0-G-1. Green Book. Issue 1. Washington, DC, USA: CCSDS, Aug. 2010

[14] K. Scott, S. Burleigh, "Bundle protocol specification", IETF RFC 5050, Nov. 2007.

[15] M. Ramadas, S. Burleigh, And S. Farrell, "Licklider Transmission Protocol—Specification", IETF Req. f. Comments RFC 5326, Sep. 2008

[16] K. Fall, "A delay-tolerant network architecture for challenged internets," ACM SIGCOMM 2003, Karlsruhe, Germany, Aug. 2003.

[17] S. Burleigh, "Delay-tolerant networking LTP convergence layer (LTPCL) adapter", draft-burleigh-dtnrg-ltpcl-02, IETF, Internet Draft, expires Feb. 2011

[18] L. Wood, W. M. Eddy, W. Ivancic, J. McKim and C. Jackson, "Saratoga: a Delay-Tolerant Networking convergence layer with efficient link utilization", Proc. of the Third Int. Work. on Satellite and Space Communications (IWSSC '07), Salzburg, Austria, September 2007.

[19] C. Moore, "Buffered Block Acknowledgement (BuBA) Protocol for Highly Errored Data Links", presentation at SPIE -conference *Defense, Security & Sensing*, Orlando, FL, April 2011

[20] B. Adamson, C. Bormann, M. Handley, and J. Macker, "NACK-Oriented Reliable Multicast (NORM) Transport Protocol," IETF, RFC 5740, Nov. 2009

[21] Proximity-1 Space Link Protocol – Rationale, Architecture, and Scenarios, Informational Report, CCSDS 210.0-G-1. Green Book. Issue 1. Washington, DC, USA: CCSDS Aug. 2007

[22] Proximity-1 Space Link Protocol – Data Link Layer, Recommended Standard, CCSDS 211.0-B-4. Blue Book. Issue 4. Washington, DC, USA: CCSDS, Jul. 2006

[23] Proximity-1 Space Link Protocol – Coding and Synchronization Sublayer, Recommendation for Space Data System Standards, CCSDS 211.2-B-1. Blue Book. Issue 1. Matera, Italy: CCSDS, Apr. 2003.